

# Quarkonia and heavy flavors at the LHC

Philippe Crochet<sup>a</sup>

Laboratoire de Physique Corpusculaire CNRS/IN2P3 F-63177 Clermont-Ferrand

Received: date / Revised version: date

**Abstract.** Perspectives for measurements of quarkonia and heavy flavors in heavy ion collisions at the LHC are reviewed.

## 1 Quarkonia and heavy flavors: what is different at the LHC

With a nucleus-nucleus center-of-mass energy nearly 30 times larger than the one reached at RHIC, the LHC will open a new era for studying the properties of strongly interacting matter at extreme energy densities [1]. One of the most exciting aspects of this new regime is the abundant production rate of hard probes which can be used, for the first time, as high statistics probes of the medium [2]. Furthermore, heavy flavor measurements at the LHC should provide a comprehensive understanding of open and hidden heavy flavor production at very low  $x$  values, where strong nuclear gluon shadowing is expected. The heavy flavor sector at LHC energies is subject to other significant differences with respect to SPS and RHIC energies. First, the large production rate offers the possibility to use a large variety of observables. Then, the magnitude of most of the in-medium effects is dramatically enhanced. Some of these aspects are discussed hereafter.

### 1.1 New observables

The Table 1 shows the number of  $c\bar{c}$  and  $b\bar{b}$  pairs produced in central A-A collisions at SPS, RHIC and LHC. From RHIC to LHC, there are 10 times more  $c\bar{c}$  pairs and 100 times more  $b\bar{b}$  pairs produced. Therefore, while at SPS only charmonium states are experimentally accessible and at RHIC it remains to be seen how much of the bottom sector can be explored, at the LHC both charmonia and bottomonia can be used, thus providing powerful probes for Quark Gluon Plasma (QGP) studies. In fact, since the  $\Upsilon(1S)$  state only dissolves significantly above the critical temperature [3], at a value which might only be reachable above that of RHIC, the spectroscopy of the  $\Upsilon$  family at the LHC should reveal unique characteristics of the QGP [4]. In addition to the centrality dependence of the  $\Upsilon$  yield, the study of the  $\Upsilon'/\Upsilon$  ratio versus transverse momentum ( $p_T$ ) is believed to be of crucial interest [4] (see below).

**Table 1.** Number of  $c\bar{c}$  and  $b\bar{b}$  pairs produced in central heavy-ion collisions ( $b = 0$ ) at SPS (Pb-Pb), RHIC (Au-Au), and LHC (Pb-Pb) energies.  $b\bar{b}$  production is negligible at the SPS.

	SPS	RHIC	LHC
$N(c\bar{c})$	0.2	10	130
$N(b\bar{b})$	–	0.05	5

On the other hand, studies with open heavy flavors also benefit from high statistics measurements. In particular, as shown in the following, the reconstruction of the  $p_T$  distribution of  $D^0$  mesons in the hadronic channel should provide valuable information on in-medium induced  $c$  quark energy loss.

### 1.2 Large quarkonium nuclear absorption

Charmonium measurements at the SPS have shown that a detailed understanding of the normal nuclear absorption is mandatory in order to reveal any anomalous suppression behavior [5]. According to Ref. [2], the following observations can be made:

- the  $J/\psi$  nuclear absorption in central Pb-Pb collisions is two times larger at the LHC than at the SPS;
- the  $J/\psi$  nuclear absorption in central Ar-Ar collisions at the LHC is similar to the one in central Pb-Pb collisions at the SPS;
- the  $\Upsilon$  nuclear absorption in central Pb-Pb collisions at the LHC is similar to the  $J/\psi$  nuclear absorption in central Pb-Pb collisions at the SPS.

### 1.3 Large resonance dissociation rate

It has been realized that, in addition to the normal nuclear absorption, the interactions with comoving hadrons and the melting by color screening, quarkonia can also be significantly destroyed by gluon ionization [6]. Since this mechanism results from the presence of quasi-free gluons,

<sup>a</sup> Philippe.Crochet@clermont.in2p3.fr

it starts being effective for temperatures above the critical temperature but not necessarily above the resonance dissociation temperature by color screening. Recent estimates [2] (see Ref. [7] for an update) of the quarkonium dissociation cross-sections show that none of the  $J/\psi$  mesons survives the deconfined phase at the LHC and that about 80 % of the  $\Upsilon$  are destroyed. Significant information about the initial temperature and lifetime of the QGP should be extracted from the  $\Upsilon$  suppression pattern.

#### 1.4 Large charmonium secondary production

An important yield of secondary charmonia is expected from  $B$  meson decays [8],  $D\bar{D}$  annihilation [9], statistical hadronization [10] and kinetic recombination [11]. Contrary to the two first processes, the two last ones explicitly assume the formation of a deconfined medium. The underlying picture is that charmonium resonances form by coalescence of free  $c$  and  $\bar{c}$  quarks in the QGP [11] or at the hadronization stage [10]. According to these models, the QGP should lead to an increase of the  $J/\psi$  yield versus centrality, roughly proportional to  $N^2(c\bar{c})$ , instead of a suppression. Due to the large number of  $c\bar{c}$  pairs produced in central heavy ion collisions at the LHC, these models predict a spectacular enhancement of the  $J/\psi$  yield; up to a factor 100 relative to the primary production yield [2, 12]. Although the statistical accuracy of the present RHIC data cannot confirm or rule out such mechanisms [13], it is interesting to extrapolate from secondary charmonium production at RHIC to secondary bottomonium production at the LHC. Indeed, the expected multiplicity of  $b\bar{b}$  pairs at the LHC is roughly equal to the expected multiplicity of  $c\bar{c}$  pairs at RHIC (Table 1). Therefore, if secondary production of charmonia is observed at RHIC, it is conceivable to expect the same formation mechanism for bottomonium states at the LHC.

#### 1.5 Complex structure of dilepton yield

The dilepton mass spectrum at the LHC exhibits new features, illustrated in Fig. 1. It can be seen that, with a low  $p_T$  threshold of around 2 GeV/ $c$  on the decay leptons, unlike-sign dileptons from bottom decay dominate the dilepton correlated component over all the mass range. These dileptons have two different origins. In the high invariant mass region, each lepton comes from the direct decay of a  $B$  meson (the so-called  $BB$ -diff channel). In the low invariant mass region, both leptons come from the decay of a single  $B$  meson via a  $D$  meson (the so-called  $B$ -chain channel). Next to leading order processes, such as gluon splitting, also populate significantly the low mass dilepton spectrum due to their particular kinematics. Then, as discussed in more detail below, a substantial fraction of the  $J/\psi$  yield arises from bottom decays. Finally, a sizeable yield of like-sign correlated dileptons from bottom decays is present. This contribution arises from the peculiar decay chain of  $B$  mesons and from  $B$  meson oscillations (see below). Its yield could be even larger than the yield of unlike-sign correlated dileptons from charm.

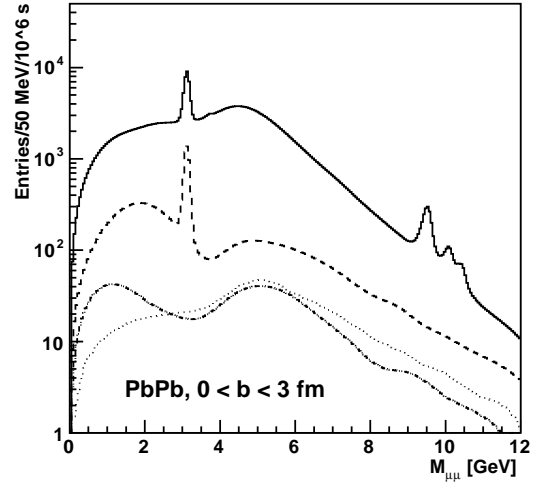


**Fig. 1.** Invariant mass spectra of dimuons produced in central ( $b < 3$  fm) Pb-Pb collisions in the ALICE forward muon spectrometer [14], with a  $p_T$  cut of 2 GeV/ $c$  applied to each single muon. The lines correspond to: like-sign correlated dimuons from bottom (dotted); unlike-sign correlated dimuons from charm (dash-dotted) and from bottom (dashed); unlike-sign correlated and unlike-sign non-correlated pairs (solid).

## 2 The LHC heavy ion program

The LHC will be operated several months per year in pp mode and several weeks in heavy-ion mode. The corresponding effective time for rate estimates is  $10^7$  s for pp and  $10^6$  s for heavy-ion operation. As described in Ref. [1], the “heavy-ion runs” include, during the first five years of operation, one Pb-Pb run at low luminosity, two Pb-Pb runs at high luminosity, one p-A run and one light-ion run. In the following years different options will be considered, depending on the first results. Three of the four LHC experiments are expected to take heavy-ion data.

### 2.1 ALICE

ALICE (A Large Ion Collider Experiment) is the only LHC experiment dedicated to the study of nucleus-nucleus collisions [15]. The detector is designed to cope with large charged particle multiplicities which, in central Pb-Pb collisions, are expected to be between 2000 and 8000 per unit rapidity at mid rapidity. The detector consists of a central barrel ( $|\eta| < 0.9$ ), a forward muon spectrometer ( $2.5 < \eta < 4$ ) and several forward/backward and central small acceptance detectors. Heavy flavors will be measured in ALICE through the electron channel and the hadron channel in the central barrel as well as through the muon channel in the forward region. Note that, contrary to the other LHC experiments, ALICE will be able to access most of the signals down to very low  $p_T$ .

### 2.2 CMS

CMS (Compact Muon Solenoid) [16] is designed for high  $p_T$  physics in pp collisions but has a strong heavy ion

program [17]. This program includes jet reconstruction, quarkonia measurements (in the dimuon channel) and high mass dimuon measurements. The detector acceptance, for quarkonia measurements, ranges from  $-2.5$  to  $2.5$  in  $\eta$ , with a  $p_T$  threshold of  $3 \text{ GeV}/c$  on single muons. Such a  $p_T$  cut still allows the reconstruction of  $\Upsilon$  states down to  $p_T = 0$  but limits  $J/\psi$  measurements to high  $p_T$ .

### 2.3 ATLAS

Like CMS, ATLAS (A Toroidal LHC ApparatuS) [18] is designed for pp physics. The detector capabilities for heavy ion physics have been investigated recently [19]. As far as heavy flavors are concerned, the physics program will focus on measurements of  $b$ -jets and  $\Upsilon$ . The detector acceptance for muon measurements is large in  $\eta$  ( $|\eta| < 2.4$ ) but, like CMS, is limited to high  $p_T$ .

## 3 Selected physics channels

### 3.1 Quarkonia

#### 3.1.1 Centrality dependence of resonance yields

The centrality dependence of the quarkonium yield, in the  $\mu\mu$  channel, has been simulated in the ALICE detector. From the results, displayed in Table 2, the following comments can be made. The statistics of  $J/\psi$  events is large and should allow for narrower centrality bins. The  $\psi'$  measurement is rather uncertain, because of the small signal to background ratio (S/B). The  $\Upsilon$  and  $\Upsilon'$  statistics and significance are quite good and the corresponding S/B ratios are almost always greater than 1. On the other hand, the  $\Upsilon''$  suffers from limited statistics. The resonances will also be measured in the dielectron channel in ALICE [20], and in the dimuon channel in CMS [17] and ATLAS [19], providing consistency cross-checks and a nice complementarity in acceptance. A recent study [21] demonstrated the capabilities of ALICE to measure the resonance azimuthal emission angle with respect to the reaction plane. Such measurements are of particular importance given the latest RHIC results on open charm elliptic flow [22].

#### 3.1.2 $\Upsilon'/\Upsilon$ ratio versus $p_T$

The  $p_T$  dependence of resonance suppression was recognized very early as a relevant observable to probe the characteristics of the deconfined medium [23]. Indeed, the  $p_T$  suppression pattern of a resonance is a consequence of the competition between the resonance formation time and the QGP temperature, lifetime and spatial extent. However, quarkonium suppression is known to result not only from deconfinement but also from nuclear effects like shadowing and absorption. In order to isolate pure QGP effects, it has been proposed to study the  $p_T$  dependence of quarkonium ratios instead of single quarkonium  $p_T$  distributions. By doing so, nuclear effects are washed out, at

**Table 2.** Preliminary yield (S), signal over background (S/B) and significance ( $S/\sqrt{S+B}$ ) for quarkonium resonances measured versus centrality in the ALICE forward muon spectrometer [14]. The input cross-sections are taken from Ref. [2]. Shadowing is taken into account. Any other suppression or enhancement effects are not included. The numbers correspond to one month of Pb-Pb data taking and are extracted with a  $2\sigma$  mass cut.

	$b$ (fm)	0-3	3-6	6-9	9-12	12-16
$J/\psi$	S ( $\times 10^3$ )	86.48	184.6	153.3	67.68	10.46
	S/B	0.167	0.214	0.425	1.237	6.243
	$S/\sqrt{S+B}$	111.3	180.4	213.8	193.4	94.95
$\psi'$	S ( $\times 10^3$ )	1.989	4.229	3.547	1.565	0.24
	S/B	0.009	0.011	0.021	0.063	0.273
	$S/\sqrt{S+B}$	4.185	6.902	8.604	9.641	7.171
$\Upsilon$	S ( $\times 10^3$ )	1.11	2.376	1.974	0.83	0.118
	S/B	2.084	2.732	4.31	7.977	12.01
	$S/\sqrt{S+B}$	27.39	41.71	40.03	27.16	10.42
$\Upsilon'$	S ( $\times 10^3$ )	0.305	0.653	0.547	0.229	0.032
	S/B	0.807	1.043	1.661	2.871	4.319
	$S/\sqrt{S+B}$	11.68	18.26	18.48	13.02	5.077
$\Upsilon''$	S ( $\times 10^3$ )	0.175	0.376	0.312	0.13	0.019
	S/B	0.566	0.722	1.18	1.936	3.024
	$S/\sqrt{S+B}$	7.951	12.55	13	9.274	3.73

least in the  $p_T$  variation of the ratio<sup>1</sup>. Following the arguments of Ref. [4], the capabilities of the ALICE muon spectrometer to measure the  $p_T$  dependence of the  $\Upsilon'/\Upsilon$  ratio in central (10%) Pb-Pb collisions have been recently investigated [24]. Two different QGP models with different system sizes were considered. The results of the simulations (Fig. 2) show that, with the statistics collected in one month of data taking, the measured  $\Upsilon'/\Upsilon$  ratio exhibit a strong sensitivity to the characteristics of the QGP. Note that in the scenario of the upper right panel of Fig. 2 the expected suppression is too large for any measurement beyond the  $p_T$  integrated one.

#### 3.1.3 Secondary $J/\psi$ from bottom decay

A large fraction of the  $J/\psi$  yield arises from the decay of  $B$  mesons. The ratio  $N(b\bar{b} \rightarrow J/\psi)/N(\text{direct } J/\psi)$  can be determined as follows. The number of directly produced  $J/\psi$  in central (5%) Pb-Pb collisions is  $0.31 [2]^2$ . The corresponding number of  $b\bar{b}$  pairs (with shadowing) amounts to  $4.56 [2]$ . The  $b \rightarrow J/\psi$  branching ratio is  $1.16 \pm 0.10\%$  [8]. Therefore  $N(b\bar{b} \rightarrow J/\psi)/N(\text{direct } J/\psi) = 34\%$  in  $4\pi$ . These secondary  $J/\psi$  mesons from  $b$  decays, which are not QGP suppressed, must be subtracted from the measured  $J/\psi$  yield prior to  $J/\psi$  suppression studies<sup>3</sup>. They can fur-

<sup>1</sup> Using ratios has the additional advantage that systematical detection inefficiencies cancel out to some extent.

<sup>2</sup> Including shadowing and no feed-down from higher states.

<sup>3</sup> In addition, 1.5% of  $B$  mesons decay into  $\chi_{c1}(1P)$  which subsequently decay into  $\gamma J/\psi$  with a 31% branching ratio [8].

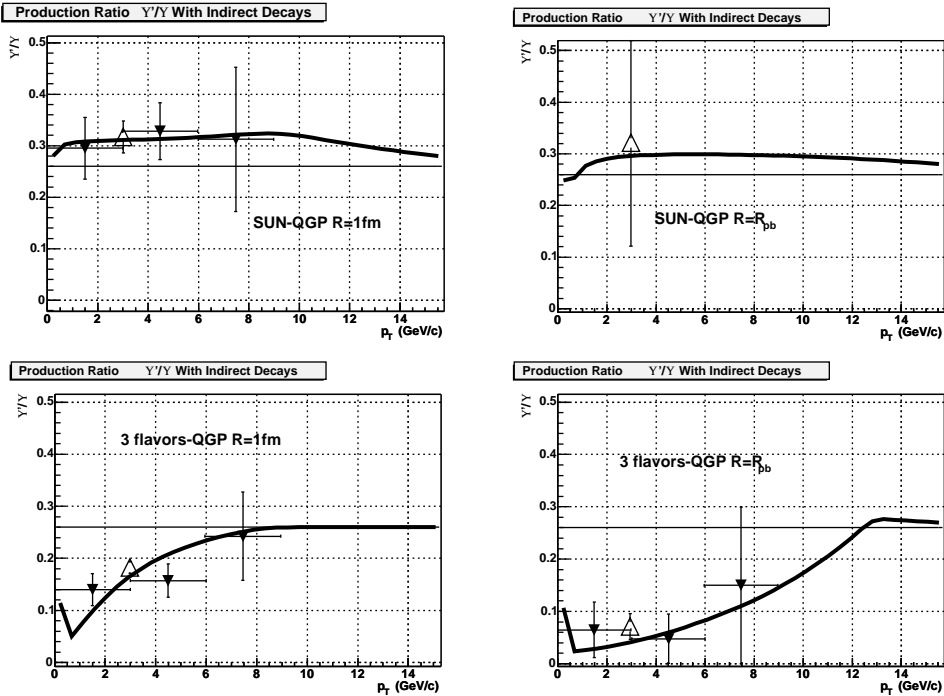


**Fig. 2.**  $\mathcal{R}'/\mathcal{R}$  ratio versus  $p_T$  for two different QGP models with different system sizes [24]. The solid curves correspond to the “theoretical ratios”. The triangles show the expected measurements with the ALICE forward muon spectrometer in one month of central (10 %) Pb-Pb data taking (the open triangles correspond to the  $p_T$  integrated ratios). Error bars are of statistical origin only. The horizontal solid lines show the expected value of the ratio in pp collisions. More details on the ingredients used in the different scenarios can be found in Ref [4].

they be used in order to measure the  $b$  cross-section in pp collisions [25], to estimate shadowing in p-A collisions and to probe the medium induced  $b$  quark energy loss in A-A collisions. Indeed, it has been shown [26] that the  $p_T$  and  $\eta$  distributions of those  $J/\psi$  exhibit pronounced sensitivity to  $b$  quark energy loss. In addition, a comparison between high mass dileptons and secondary  $J/\psi$  distributions could clarify the nature of the energy loss [26].

Due to the large life-time of  $B$  mesons,  $J/\psi$  from bottom decay is the only source of  $J/\psi$  not coming from the primary vertex<sup>4</sup>. The best way to identify them is, therefore, to reconstruct the invariant mass of dileptons with displaced vertices i.e. with impact parameter,  $d0$ , above some threshold. Simulations have shown that such measurements can successfully be performed with dielectrons measured in the central part of ALICE using the ITS, the TPC and the TRD [20] and with dimuons in CMS [26], thanks to the excellent spatial resolution of the inner tracking devices of these experiments. It should also be possible to disentangle the two sources of  $J/\psi$  from the slopes of the overall measured  $J/\psi$   $p_T$  distributions since primary  $J/\psi$  have a harder spectrum [20]. Finally, a recent study [27] has demonstrated the possibility to isolate  $J/\psi$  from bottom decay in pp collisions, without secondary ver-

tex reconstruction, by triggering on three muon events in the ALICE forward muon spectrometer. Indeed, in standard (dimuon) pp events, the  $J/\psi$  peak contains 85% of primary  $J/\psi$  and 15% of  $J/\psi$  from  $B$  meson decays. The situation is totally inverted in tri-muon events because a  $B\bar{B}$  pair can easily produce many decay leptons. In such events the  $J/\psi$  peak contains 85% of secondary  $J/\psi$  from bottom decay and 15% of direct  $J/\psi$  [27]. It is obvious that this analysis technique becomes less and less efficient as the track multiplicity increases. Nevertheless, it could still be performed for light-ion systems.

## 3.2 Open heavy flavors

### 3.2.1 Open bottom from single leptons with displaced vertices

As mentioned above, the  $d0$  distributions of leptons from heavy meson decays exhibit a significantly large tail because heavy mesons have a larger life-time than other particles decaying into leptons. Therefore, inclusive measurements of open heavy flavors can be achieved from the identification of the semi-leptonic decay of heavy mesons [20]. Recent simulation studies [28] performed with the ALICE central detectors show that with  $d0 > 180 \mu\text{m}$  and  $p_T > 2 \text{ GeV}/c$ , the monthly expected statistics of electrons from  $B$  decays in central Pb-Pb collisions is  $5 \cdot 10^4$

<sup>4</sup>  $J/\psi$  from statistical hadronization, kinetic recombination and  $D\bar{D}$  annihilation are usually quoted as secondary  $J/\psi$  but they originate from the primary vertex.

with a contamination of only 10 %, mainly coming from charm decays. The deconvolution of  $d0$  distributions by imposing different  $p_T$  cuts should allow charm measurements as well. Furthermore, such analyses should give access to the  $p_T$  distribution of  $D$  and  $B$  mesons by exploiting the correlation between the  $p_T$  of the decay lepton and that of its parent [20].

### 3.2.2 Open bottom from single muons and unlike-sign dimuons

The possibility to measure the differential  $B$  hadron inclusive production cross-section in central Pb-Pb collisions at the LHC has recently been investigated by means of analyses similar to the ones performed in pp collisions at the Tevatron. This study is based on unlike-sign dimuon mass and single muon  $p_T$  distributions measured with the ALICE forward muon spectrometer [29]. The principle is first to apply a low  $p_T$  threshold on single muons in order to reject background muons (mainly coming from charm decays) and therefore to maximize the  $b$  signal significance. Then, fits are performed to the total (di)muon yield with fixed shapes for the different contributing sources and the bottom amplitude as the only free parameter. The  $B$  hadron production cross-section is then obtained after corrections for decay kinematics and branching ratios and muon detection acceptance and efficiencies. This allows to extract the signal over a broad range in  $p_T$  (Fig. 3). A large statistics is expected [29] thus allowing detailed investigations on  $b$  quark production mechanisms and in-medium energy loss. On the other hand, such a measurement, which can be performed for different centrality classes, provides the most natural normalization for  $\mathcal{Y}$  suppression studies.

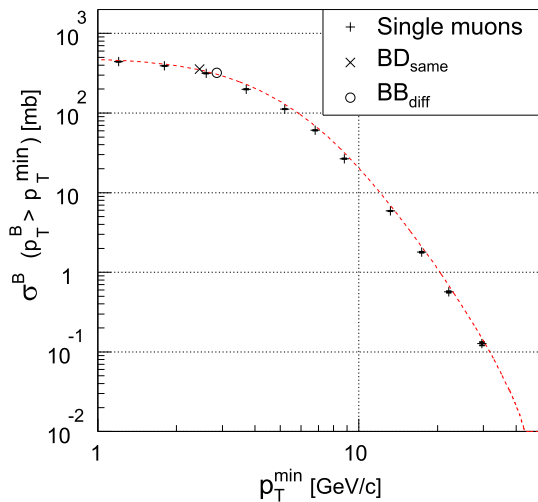


**Fig. 3.** Differential  $B$  hadron inclusive production cross-section in the most central (5 %) Pb-Pb collisions [29]. Measurements from unlike-sign dimuons at low and high mass and from single muons (symbols) are compared to the input distribution (curve). Statistical errors (not shown) are negligible.

### 3.2.3 Open bottom from like-sign dileptons

As shown in Fig. 1, a sizable fraction of like-sign correlated dileptons arise from the decay of  $B$  mesons. These dileptons have two different origins:

- The first decay generation of  $B$  mesons contains  $\sim 10\%$  of primary leptons and a large fraction of  $D$  mesons which decay semi-leptonically with a branching ratio of  $\sim 12\%$ . Therefore a  $B\bar{B}$  pair is a source of like-sign correlated dileptons via channels like:
 
$$B^+ \rightarrow \bar{D}^0 e^+ \nu_e, \bar{D}^0 \rightarrow e^- \text{ anything}$$

$$B^- \rightarrow D^0 \pi^-, D^0 \rightarrow e^+ \text{ anything}$$
 where the  $B^+B^-$  pair produces a correlated  $e^+e^+$  pair in addition to the two correlated  $e^+e^-$  pairs;
- The two neutral  $B^0\bar{B}^0$  meson systems  $B_d^0\bar{B}_d^0$  and  $B_s^0\bar{B}_s^0$  undergo the phenomenon of particle-antiparticle mixing (or oscillation). The mixing parameters<sup>5</sup> are  $\chi_d = 0.17$  and  $\chi_s \geq 0.49$  [8]. Therefore, a  $B_d^0\bar{B}_d^0$  ( $B_s^0\bar{B}_s^0$ ) pair produces, in the first generation of decay leptons, 70 % (50 %) of unlike-sign correlated lepton pairs and 30 % (50 %) of like-sign correlated lepton pairs.

This component is accessible experimentally from the subtraction of so-called event-mixing spectrum from the like-sign spectrum [30]. The corresponding signal is a reliable measurement of the bottom cross-section since i)  $D$  mesons do not oscillate [8] and ii) most (if not all) leptons from the second generation of  $D$  meson decay can be removed by a low  $p_T$  threshold of about 2 GeV/ $c$ .

### 3.2.4 Hadronic charm

In the central part of ALICE, heavy mesons can be fully reconstructed from their charged particle decay products in the ITS, TPC and TOF [31]. Not only the integrated yield, but also the  $p_T$  distribution can be measured. The most promising decay channel for open charm detection is the  $D^0 \rightarrow K^- \pi^+$  decay (and its charge conjugate) which has a branching ratio of 3.8 % and  $c\tau = 124 \mu\text{m}$ . The expected rates (per unit of rapidity at mid rapidity) for  $D^0$  (and  $\bar{D}^0$ ) mesons, decaying in a  $K^\mp \pi^\pm$  pair, in central (5 %) Pb-Pb at  $\sqrt{s} = 5.5$  TeV and in pp collisions at  $\sqrt{s} = 14$  TeV, are  $5.3 \cdot 10^{-1}$  and  $7.5 \cdot 10^{-4}$  per event, respectively. The selection of this decay channel allows the direct identification of the  $D^0$  particles by computing the invariant mass of fully-reconstructed topologies originating from displaced secondary vertices. The expected statistics are  $\sim 13\,000$  reconstructed  $D^0$  in  $10^7$  central Pb-Pb collisions and  $\sim 20\,000$  in  $10^9$  pp collisions. The significance is larger than 10 for up to about  $p_T = 10$  GeV/ $c$  both in Pb-Pb and in pp collisions. The cross section can be measured down to  $p_T = 1$  GeV/ $c$  in Pb-Pb collisions and down to almost  $p_T = 0$  in pp collisions.

The reconstructed  $D^0$   $p_T$  distributions can be used to investigate the energy loss of  $c$  quarks by means of the

<sup>5</sup> Time-integrated probability that a produced  $B_d^0$  ( $B_s^0$ ) decays as a  $\bar{B}_d^0$  ( $\bar{B}_s^0$ ) and vice versa.

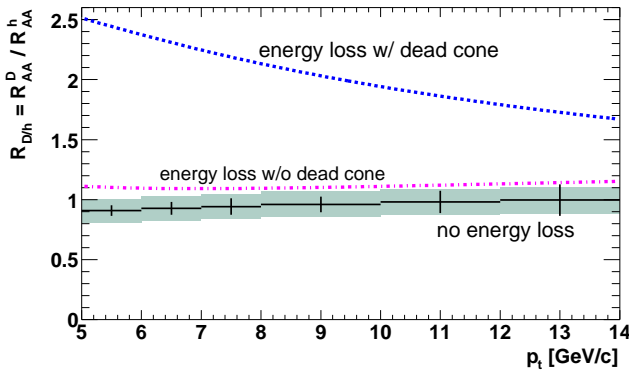


**Fig. 4.** Ratio of the nuclear modification factors for  $D^0$  mesons and for charged (non-charm) hadrons with and without energy loss and dead cone effect [32]. Errors corresponding to the case “no energy loss” are reported. Vertical bars and shaded areas correspond to statistical and systematic errors, respectively.

nuclear modification factor  $R_{AA}^{D^0}$  [31, 32]. Even more interesting is the ratio of the nuclear modification factors of  $D^0$  mesons and of charged (non-charm) hadrons ( $R_{D/h}$ ) as a function of  $p_T$ . Apart from the fact that many systematic uncertainties on  $R_{AA}^{D^0}$  cancel out with the double ratio,  $R_{D/h}$  offers a powerful tool to investigate and quantify the so-called dead cone effect (Fig. 4).

### 3.2.5 Electron-muon coincidences

The semi-leptonic decay of heavy mesons involves either a muon or an electron. Therefore, the correlated  $c\bar{c}$  and  $b\bar{b}$  cross-sections can be measured in ALICE from unlike-sign electron-muon pairs where the electron is identified in the central part and the muon is detected in the forward muon spectrometer. The  $e\mu$  channel is the only leptonic channel which gives a direct access to the correlated component of the  $c\bar{c}$  and  $b\bar{b}$  pairs. Indeed, in contrast to  $e^+e^-$  and  $\mu^+\mu^-$  channels, neither a resonance, nor direct dilepton production, nor thermal production can produce correlated  $e\mu$  pairs. Within ALICE, the  $e\mu$  channel has the additional advantage that the rapidity distribution of the corresponding signal extends from  $\sim 1$  to  $\sim 3$ , therefore bridging the acceptances of the central and the forward parts of the detector [33]. Electron-muon coincidences have already been successfully measured in pp collisions at  $\sqrt{s} = 60$  GeV [34] and in p-nucleus collisions at  $\sqrt{s} = 29$  GeV [35]. Preliminary simulations have shown the possibility, with ALICE, to measure the correlated  $e\mu$  signal after appropriate background subtraction [36].

## 4 Summary

The heavy flavor sector will bring fantastic opportunities for systematic explorations of the dense partonic system formed in heavy ion collisions at the LHC through a wide variety of physics channels. In addition to the channels discussed here, further exciting possibilities should be opened

with, for example, charmed baryons, high mass dileptons, quarkonia polarization and dilepton correlations.

## Acknowledgments

I am grateful to A. Andronic, M. Bedjidian, A. Dainese, S. Grigoryan, R. Guernane, G. Martinez and A. Morsch for their help in preparing this paper.

## References

1. F. Carminati *et al.*, J. Phys. **G30** (2004) 1517.
2. M. Bedjidian *et al.*, arXiv:hep-ph/0311048.
3. S. Digal, P. Petreczky and H. Satz, Phys. Rev. **D64** (2001) 094015; C. Y. Wong, Phys. Rev. **C65** (2002) 034902.
4. J. F. Gunion and R. Vogt, Nucl. Phys. **B492** (1997) 301.
5. L. Kluber, these proceedings and references therein.
6. X. M. Xu, D. Kharzeev, H. Satz and X. N. Wang, Phys. Rev. **C53** (1996) 3051.
7. D. Blaschke, Y. Kalinovsky and V. Yudichev, Lect. Notes Phys. **647** (2004) 366.
8. S. Eidelman *et al.*, Phys. Lett. **B592** (2004) 1.
9. C. M. Ko, B. Zhang, X. N. Wang and X. F. Zhang, Phys. Lett. **B444** (1998) 237; P. Braun-Munzinger and K. Redlich, Eur. Phys. J. **C16** (2000) 519.
10. P. Braun-Munzinger and J. Stachel, Phys. Lett. **B490** (2000) 196.
11. R. L. Thews, M. Schroedter and J. Rafelski, Phys. Rev. **C63** (2001) 054905.
12. A. Andronic, P. Braun-Munzinger, K. Redlich and J. Stachel, Phys. Lett. **B571** (2003) 36.
13. R. Thews, these proceedings.
14. S. Grigoryan, private communication (2004).
15. <http://alice.web.cern.ch/Alice/AliceNew/>.
16. <http://cmsinfo.cern.ch/Welcome.html/>.
17. G. Baur *et al.*, CMS-NOTE-2000-060 (2000).
18. <http://atlas.web.cern.ch/Atlas/>.
19. ATLAS Coll., CERN/LHCC **2004/009** (2004).
20. ALICE Coll., CERN/LHCC **99-13** (1999).
21. A. Morsch *et al.*, ALICE-INT-**2001-22** (2001).
22. S. Kelly, J. Phys. **G30** (2004) S1189.
23. J. P. Blaizot and J. Y. Ollitrault, Phys. Lett. **B199** (1987) 499; F. Karsch and H. Satz, Z. Phys. **C51** (1991) 209.
24. E. Dumonteil, Thèse de doctorat de l’Université de Caen, (2004), <http://tel.ccsd.cnrs.fr/>; E. Dumonteil and P. Crochet, ALICE-INT-2005-002 (2005).
25. D. Acosta *et al.*, arXiv:hep-ex/0412071.
26. I. P. Lokhtin and A. M. Snigirev, Eur. Phys. J. **C21** (2001) 155.
27. A. Morsch, private communication (2004).
28. M. Lunardon and R. Turrisi, in preparation.
29. R. Guernane *et al.*, in preparation.
30. P. Crochet and P. Braun-Munzinger, Nucl. Instrum. Meth. **A484** (2002) 564.
31. A. Dainese, arXiv:nucl-ex/0311004.
32. A. Dainese, Eur. Phys. J. **C33** (2004) 495.
33. Z. Lin and R. Vogt, Nucl. Phys. **B544** (1999) 339.
34. A. Chilingarov *et al.*, Phys. Lett. **B83** (1979) 136.
35. T. Akesson *et al.*, Z. Phys. **C72** (1996) 429.
36. ALICE Coll., CERN/LHCC 99-22 (1999).